Isı Bilimi ve Tekniği Dergisi, 44, 1, 129-142, 2024
J. of Thermal Science and Technology
©2024 TIBTD Printed in Turkey
ISSN 1300-3615
e-ISSN 2667-7725
https://doi.org/10.47480/isibted.1494159

EXPERIMENTAL STUDY OF DELAYING THE STALL OF THE NACA 0020 AIRFOIL USING A SYNTHETIC JET ACTUATOR ARRAY WITH DIFFERENT ORIFICE GEOMETRIES

Esra TÜREN*, Hakan YAVUZ*
* Çukurova University Engineering Faculty, Mechanical Engineering Department 01330, Adana, TURKEY
essraturen@gmail.com, ORCID: 0000-0002-2863-6444
hyavuz@cu.edu.tr, ORCID: 0000-0002-6166-0921

(Geliş Tarihi: 06.08.2023, Kabul Tarihi: 06.05.2024)

Abstract: An experimental study on the effect of active flow control using a synthetic jet mechanism on stall delay for the NACA 0020 airfoil is conducted. The experiments are carried out at an open-suction type wind tunnel at Reynolds number $5x10^4$. In the presented experimental study, aerodynamic force measurements of the airfoil with having different orifice geometries (cylindrical, rectangular, sinusoidal, v-type, inclined rectangular) are examined by using a speaker type actuator in synthetic jet mechanism. It is observed that all different orifice geometries are effective in delaying the stall angle of NACA 0020 airfoil. However, it is observed that the inclined rectangular type of synthetic jet geometry is the most advantageous in delaying the stall of the airfoil. The effects of geometric parameters of the actuator on lift and drag coefficient of the NACA0020 airfoil are investigated. Experimental results show that among the all-orifice geometries the rectangular orifice geometry is the most effective in increasing lift coefficient of the airfoil. It is observed that there is a maximum decrease in drag at 10° where the stall occurs. In addition, the decrease in drag is observed after 10° in rectangular, v-type and inclined rectangular orifice geometries.
Keywords: Active flow control, synthetic jet, NACA0020 airfoil, drag and lift coefficient, stall shifting

FARKLI DELİK GEOMETRİSİNE SAHİP SENTETİK JET AKTÜATÖR DİZİSİ KULLANARAK NACA 0020 HAVA FOLYOSUNUN DURUŞUNUN GECİKTİRİLMESİNE YÖNELİK DENEYSEL ÇALIŞMA

Özet: NACA 0020 kanat profili üzerinde sentetik jet mekanizması için aktif akış kontrolünün stall gecikmesi üzerindeki etkisi hakkında deneysel bir çalışma gerçekleştirilmiştir. Deneyler 5x104 Reynolds sayısında açık emişli tip rüzgar tünelinde gerçekleştirilmiştir. Sunulan deneysel çalışmada, sentetik jet mekanizmasında hoparlör tipi bir aktüatör kullanılarak farklı orifis geometrilerine (silindirik, dikdörtgen, sinüzoidal, v-tipi, eğimli dikdörtgen) sahip kanadın aerodinamik kuvvet ölçümleri incelenmiştir. Tüm farklı orifis geometrilerinin NACA 0020 kanadının stall açısını geciktirmede etkili olduğu gözlemlenmiştir. Ancak eğimli dikdörtgen tip sentetik jet geometrisinin kanadın stall açısını geciktirmede en avantajlı olduğu gözlemlenmiştir. Aktüatörün geometrik parametrelerinin NACA0020 kanadının kaldırma ve sürükleme katsayısı üzerindeki etkileri araştırılmıştır. Deneysel sonuçlar, tüm delikli geometriler arasında dikdörtgen delikli geometrinin kanadın kaldırma katsayısını arttırmak için en etkili olduğunu göstermektedir. Stall' un meydana geldiği 10°'de sürüklemede maksimum azalma olduğu gözlemlenmiştir. Ayrıca dikdörtgen, v-tipi ve eğimli dikdörtgen orifis geometrilerinde 10°'den sonra sürüklemede azalma olduğu gözlenmiştir.
Anahtar Kelimeler: Aktif akış kontrolü, sentetik jet, NACA0020 kanat profili, sürükleme ve kaldırma katsayısı, durma kayması

NOMENCLATURE

F_L	Lift force
F_D	Drag force
C_D	Drag coefficient
C_L	Lift coefficient
D	Diameter of the cylinder [mm]
ρ	Fluid density [kg/m^3]
μ	Fluid dynamic viscosity [kg/(m.s)
Re	Reynolds number [=$U_0\rho D/\mu$]
U_0	Free stream velocity [m/s]
A	Airfoil area [mm^2]
f	Excitation frequency [kHz]

INTRODUCTION

Throughout history, people have experimented with the dream of flying through the air. With the beginning of human flight in the 18th century, many researchers tried to increase the lift force and reduce the drag force by making changes to the aircraft's structure and configuration, aiming to improve the aerodynamic performance of the system Therefore, the flow control applications are used to delay or prevent undesirable situations occurring in the flow. The aerodynamic flow control is initially defined by Gad-el-Hak (2000) as a method of appropriately changing the natural shape or character of a desired section of a flow field. The flow control methods cause changes in many factors such as increase in lift, decrease in drag, delaying flow separation etc. contributing to its aerodynamic performance.

Mainly, the flow control methods are classified as active and passive methods (Genç et al. 2012; Joshi and Gujarathi, 2016). The active or passive flow control methods aim to change the flow field on an aerodynamic body by using various techniques (Traub et al. 2004). The passive control technique is a method that does not require any external power. For example, vortex generators, roughness, hump, groove and tip blade type airfoil modification are defined as passive flow control methods. Since passive flow control methods do not utilize an external power, they cannot adjust the components that change according to variable flow conditions, such as different angles of attack and Reynolds numbers, under desired conditions. The active flow control techniques are methods that require an additional power source. The active flow controllers have many advantages in terms of increasing efficiency in obtaining data at the right time and reducing power consumption of control systems. The biggest advantage compared to passive flow control methods is that they can adjust actuators according to the changing variables in the desired conditions. The piezoelectric, acoustic (loudspeaker) and piston-cylinder mechanisms are used as actuators in synthetic jet, which is one of the active flow control applications. Mallinson et al. (2004), a piezoelectric diaphragm and a speaker created using a piston-cylinder mechanism as the moving surface were investigated. Frequency and amplitude variation types of actuators such as piston cylinder, speaker and piezoelectric diaphragm have generally been created for such purposes. In the piston-cylinder mechanism, the frequency is lower and the amplitude is larger. However, in piezoelectric diaphragms the frequency is high and the amplitude is very low. The advantage of the speaker is about its fast response time and controllability as a synthetic jet mechanism, which is preferred in flow control applications. Zhao et al. (2016) investigated experimentally using speakers as actuators in synthetic jet arrays. As a result of this experimental study, it is seen that synthetic jet arrays are effective in delaying the flow separation. It is also observed that it contributes to delaying the airfoil stalling. Pulsed jet is an unstable type of a jet. Because they need an additional flow source and produce instantaneous high velocity in the exit gap. Pulsed jets can be created as fast-acting solenoid valves, high-speed rotary sounder valves or structures with rotating cavities (Critten et al, 2001). Fibre composite materials occur by changing the shape of airfoil. It contributes to improving aerodynamic performance in different flight conditions. However, the morphing aircraft wings created with fibre composite materials always have disadvantages in terms of cost, complexity or weight (Barbarino et al., 2011) In their study, Ahuja and Burrin (1984) used it to control the flow of signal generation in a given Reynolds number and angle of attack for specific frequency generation in an audio source connected to an amplifier. The synthetic jets, which are one of the active flow control methods, attract the attention of researchers because of their wide application area. The Synthetic jet mechanisms are used for many different purposes such as heat transfer (Youmin et al. 2014), mixing vessels (Qingfeng et al. 2013), cooling of electronic devices (Chaudhari et al. 2010), separation control in aircraft wings (Gillarranz et al. 2005), (Holman et al. 2003), increase in lift (Kim a Kim, 2009), reduction in friction force (He et al. 2001), boundary layer control (You and Moin. 2008) and stall control (Yen and Ahmed 2012). An important advantage of the synthetic jet mechanism is that it has a simple working principle in which the liquid is sucked and blown by the forward and backward movement of the cavity diaphragm in an open pipe or channel. In the periodic flow movement that occurs here, the fluid forms a vortex ring in the cavity during blowing. This vortex ring spreads outward at its own speed. During suction, this liquid is drawn back into the cavity. By repeating this periodic motion, synthetic jets are formed.

Studies of synthetic jet mechanisms began in the 1950s with the study of acoustic flow by Ingard and Labate (1950). Later, as synthetic jet studies became more widespread as studies in this field expanded in the late 20th century. Smith and Glezer (1998) carried out extensive studies on this subject and introduced the term 'Synthetic Jet' to the literature. After the 21st century, numerical and experimental studies on the structures of synthetic jets have become widespread (Trávníček 2005). The use of loudspeakers in synthetic jets is preferred because it is easy to integrate into the system and has a short response time. The synthetic jet mechanism is affected by the actuator, its geometric form and related fluid parameters (Hong, 2020). Zhang et al., (2015) numerically examined the frequency variation of the actuator parameters of the synthetic jet mechanism. In the models created in their study, it was observed that the heat transfer has increased with the increase in the frequency. Feero et al. (2015) examined the effect of jet structure in the orifice of a change in the diaphragm cavity. In this study, the performance of cylindrical, conical and curvilinear contraction structures in the cavity structure of the diaphragm was investigated. As a result of the study, it was observed that the cavity oscillation had the best performance in the curvilinear cavity. Although the synthetic jet mechanism is relatively

new active flow control method, it has been observed that it is an effective method in many areas such as flow separation around the wing, shifting the stall angle, and increase in lift and decrease in drag. In a study by Seifert et al. (1996), a synthetic jet mechanism, which is one of the active flow control applications, was used for the NACA 0015 airfoil. In this study, it reported that synthetic jet mechanism was effective in delaying the stall. Hassan (2006) numerically investigated the stall control in a two-actuated jet array used in the airfoil. As a result of the study, it is determined that when the existing two-point hybrid active flow control strategy is used instead of a single point at a certain angle of attack of the airfoil in the jet array, the improvement post-stall lift-drag ratio. Amitay et al. (2001) investigated flow separation using synthetic jet actuators on a symmetrical airfoil. It has been observed that the momentum required to recombine the separated air decreases as the actuator approaches the separation point. Zhang and Zhong (2009) observed flow control in water by creating a series of circular synthetic jet structures in the airfoil. In their study, a laser-induced fluorescence was used for flow visualization. It has been determined that in separated flow, flow separation occurs in two or three high flow velocity lines.

Collins and Zelenevitz (1975) studied the Reynols number between 25000 and 53000 using a synthetic jet mechanism in an airfoil. A loudspeaker was placed on the surface of the airfoil. The experiments were performed by generating a constant sound wave until partial bonding occurred. As a result of the experiments, it was observed that the lift greatly increased as the amplitude value of the acoustic stimulation increased. Zaman and McKinzie (1991) studied the acoustic effect in a two-dimensional airfoil with Reynolds number between 25 000 and 100 000. The Smoke wire flow visualization and hot-wire anemometry were used to support the experimental setup. In addition, in this study, frequency variation was investigated by keeping the excitation amplitude constant. In the experimental results, it is observed that there is an increase in the C_L lift coefficient. Yarusevych et al. (2003) studied acoustic excitation in a NACA 0025 airfoil at Reynolds numbers 57 000, 100 000 and 150 000 and at three different angles of attack (0, 5 and 10 degrees). In the study, a hot wire anemometer was used for velocity measurements. As a result of the experiment, it was observed that the optimum frequency and amplitude values of acoustic stimulation varied depending on the Reynolds number and attack angles. Guaqing et al. (2016) experimentally investigated the NACA 0025 airfoil on the airfoil using the synthetic jet mechanism from the active flow control method. In this study, they examined the effect on synthetic jet locations. In addition, the effect of the angle change in the synthetic jet inlet was investigated. As a result, jets located close to the front of the airfoil were more advantageous in delaying the stall. In addition, it has been determined that the performance of jet arrays in flow control application is more effective than single actuator performances. Moreover, it has been observed that the aerodynamic performance of the lifting force has been improved.

In this study, one of the active flow control applications is used to examine the flow control effects of Reynolds number 50 000 on the NACA 0020 airfoil in a synthetic jet mechanism using a loudspeaker as an actuator. In addition, in this study, it is aimed to investigate the contribution of the flow control around the airfoil of the orifice jet geometries named in five different structures as cylindrical, rectangular, sinusoidal, V-type and inclined rectangular. The experimental study is carried out in an open suction wind tunnel. It is aimed that different orifice jet geometries can shifting the stall angle formed on the airfoil and contribute to aerodynamic properties such as improvements in drag, lift force and stall.

EXPERIMENTAL SETUP

Airfoil Model and Synthetic Jet Design

In this study, 40 mm loudspeakers are used as the synthetic jet mechanism as shown in Figure 1. In this experimental study, five different models are selected to examine the effects of the jet structures in different orifice geometries of the synthetic jet mechanism. The orifice models of the synthetic jet mechanism are determined as circular, rectangular, sinusoidal, V-type and inclined rectangular. The circular (Lee et al. 2012 and Zhao et al. 2016) and rectangular (Abdou et al. 2006) orifices are used in the literature. In addition, three new different geometries are also used as namely as sinusoidal, V-type and inclined rectangular to control the flow around the airfoil. Figure 2 shows orifice geometries in different geometries. When Guoqing et al. (2016) examined the position of the synthetic jet mechanism in their study; maximum lift coefficient and stall were observed when it was close to the leading edge. In this study, considering the airfoil and the dimensions of the speaker, it is positioned at approximately %21 of the chord as the closest position to the leading edge.

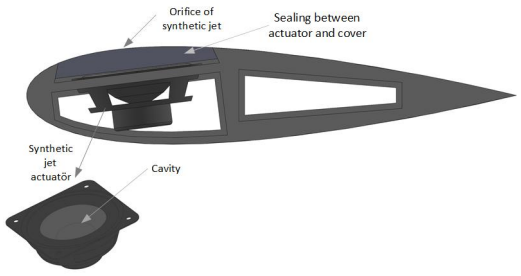

Figure 1. Assembly of the jet actuator in the airfoil model

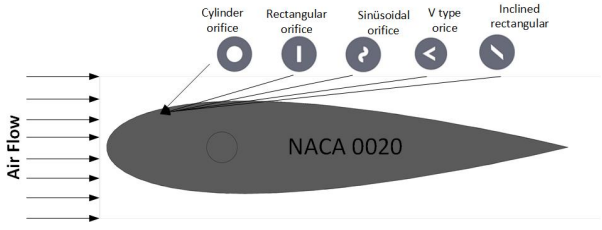

Figure 2. Design of 5 different orifice geometric models in a synthetic jet actuator

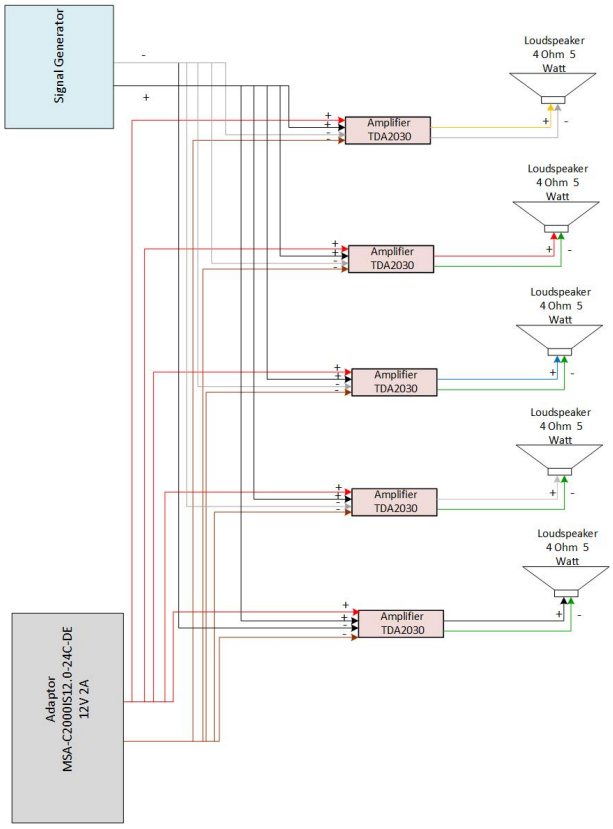

a.

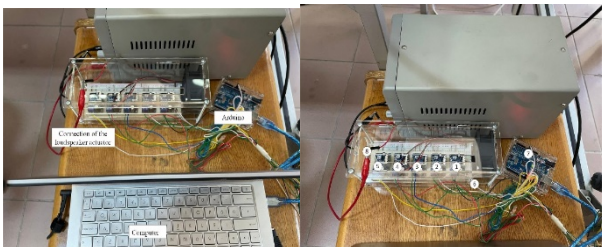

b. **c.**

Figure 3. The loudspeaker used as the actuator in the synthetic jet mechanism **a.** Systematic wiring diagram **b.** Connection equipment in the experimental setup **c.** Illustration of each connection of the speaker actuator

In the study of Paula et al. (2017), NACA0012, NACA0020 and NACA0030 airfoils were examined at low Reynolds number (MAV and UAV operating conditions). As a result of the study, it was seen that although the profile drag increases as the wing thickness increases in airfoil design, thicker airfoils are more suitable in terms of maximum lift values. In the light of this study, the selection of the NACA 0020 airfoil model was also made by taking into account the dimensions of the actuator, the assembly of the actuator arrays and the location of the actuators at low Reynolds number (MAV and UAV operating conditions). NACA 0020 airfoil model is designed with a span length of 300 mm and a chord length of 150 mm. In design of the wind, five 40 mm-long speakers, are used as synthetic jet actuator array, are placed on the airfoil profile at equal intervals. Figure 3a shows the loudspeaker electrical connection diagram. Figure 3b shows the connection of the system to the computer and the Arduino. In Figure 3c, each connection of the loudspeaker actuator is numbered. In Figure 3c, all green, and white cables were connected to the "-" output of each amplifier for speaker connection in connections 1, 2, 3, 4, and 5, respectively. Black, white, blue, red and yellow 22 AWG cables were connected to the "+" output respectively. Connection cable number 6 is brown coloured to the "-" output of the adapter, and a red cable is connected to the "+" output. Arduino Uno is used as the signal driver in the speaker connection circuit. The circuit is completed by connecting a grey cable to the GND input at connection number 7 and a white cable to pin number 10. In order to prevent the amplifiers from overheating, a 12V 2A fan has been added to the system. Finally, the operating frequency of the experiment (Türen and Yavuz, 2023) is created at 2, 4 and 8 Hz, with a constant pulse width of 1%.

The NACA 0020 airfoil is selected, taking into account the size of the actuator and the placement of the actuator arrays in the airfoil model. The NACA 0020 airfoil is designed by taking the chord length as 150 mm and the span length as 300 mm. The first design of the NACA 0020 aircraft wing is modelled in the Computer Aided Design (CAD) software, as seen in Figure 4.

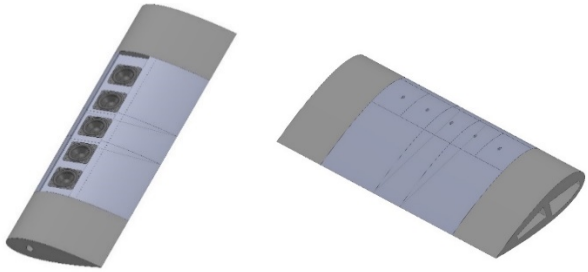

a. **b.**

Figure 4. a. Loudspeaker placement image of NACA 0020 airfoil in CAD software **b.** Image of top cover designs of NACA 0020 airfoil in CAD software

Then, the parts of the designed airfoil profile are produced by using a Three-Dimensional Printer (3D printer). There are parts of the airfoil as seen in Figure 5. After the airfoil model is produced on a 3D printer, its surface is first sanded with P320 sandpaper. Then, polyester body filler is applied to the model surface and the airfoil is mounted. The model surface is finally sanded smooth with P2000 sandpaper. Finally, the smoothness is achieved by painting the model. Table 1 shows the parameters of the airfoil in the experiment and the loudspeaker used as a synthetic jet actuator.

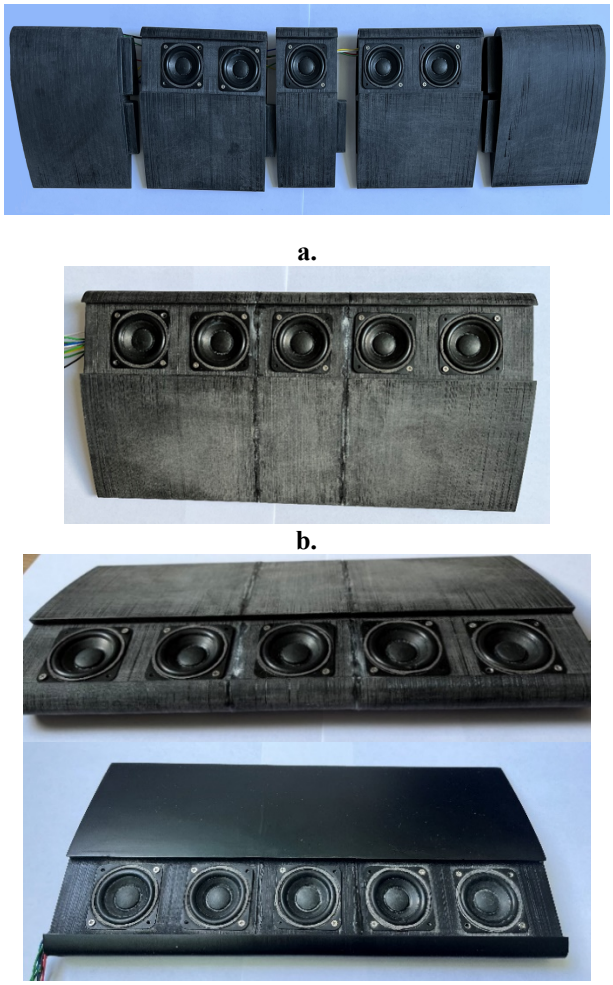

a.

b.

c.

Figure 5. NACA 0020 airfoil a. Pre-assembly view of loudspeakers and cables b. Assembled top view c. Assembled side view and airfoil assembly image without slides

Table 1. Parameters of airfoil and jet actuator

PARAMETERS	VALUE
Chord x Span (mm)	150 x 300
Width x lenght of jet orifice (mm)	0.5 x 2
Size of jet actuator (mm^3)	40 x 40 x 18
Resistance of actuator (Ω)	4
Rated power of actuators (W)	5

Wind Tunnel

The experiments are carried out in the wind tunnel located in the Aerodynamics Research Laboratory of Niğde Ömer Halisdemir University, Department of Mechanical Engineering. This wind tunnel is an open suction type wind tunnel with the test section having a cross section of 570 mm x 570 mm and a length of 1000 mm. The experiments on flow control around the NACA 0020 airfoil are carried out in a wind tunnel at a Reynolds number of 50000 and a free stream speed of 6.2 m/s. Starting from the entrance of the test area in the wind tunnel, speed scanning is carried out in horizontal and vertical directions using a hot wire anemometer (Dantec Multichannel CTA and 55P11 probe). Turbulence intensity is found to be around 0.5% in the region outside the boundary layer region where uniform velocity distributions are obtained. The experimental setup of the wind tunnel is shown in Figure 6. NACA 0020 The chord length and span length of the airfoil are defined as 150 and 500 mm, respectively. Two end plates are used and their diameter is chosen as 300 mm. The wing profile is mounted in the wind tunnel section made of Plexiglas material.

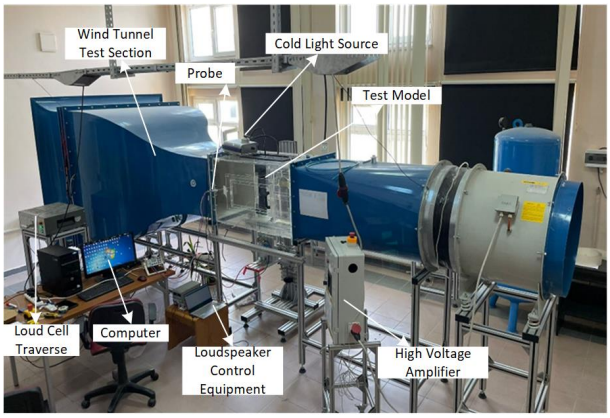

Figure 6. Wind tunnel experimental setup

In the 3D printer, the main body of the airfoil model is produced from PLA+ filament with 1.75 mm diameter. In addition, end plates made of Plexiglas material is added to the two ends of the airfoil model and the whole model is assembled. As seen in Figure 7, the airfoil is placed vertically on the test setup in the wind tunnel.

Force Measurement

ATI Gamma model six-axis load force is used to measure the drag and lift force of the test model. It is mounted on a computer-controlled rotating unit to measure the angle of attack of the test model. Measurements are taken at a sampling frequency of 300 Hz and the average of every 100 measurements is taken to record 3 measurements per second. The measurements lasted 25 seconds and 2500 data are taken for each experiment. These experiments are repeated twice in each experimental session. Angle of attacks for the force measurement is varied between 0° and 18° with an increment of 1°. Uncertainty for the force measurement is calculated to be lower than ±3%. The experiments are repeated and hence the error rate is minimized. To determine the net forces acting on the airfoil, the connection plates between the end plates, retaining rod and model are subtracted from the total force. Considering the interface effect, the forces acting on the retaining rod and the lower end plate are measured together. The test model, consisting of the upper end plates, the airfoil model and the connecting elements between the model, the bottom end plate and the retaining rod, is prepared and mounted in the test section of the wind tunnel. As a result of these measurements, the force

acting on the lower end plate is calculated. The force acting on the bottom end plate is also considered as the force acting on the upper end plate. As a result of these experimental studies, the net force acting on the airfoil is determined based on the interface effect. These experimental steps are repeated for all angles of attack. Lift force was defined as

$$F_L = \frac{1}{2} \rho . U_0^{\,2} A . C_L \quad (1)$$

ρ is the density of the fluid flowing in the tunnel, U_0 is the free stream velocity of the fluid flowing in the tunnel, A is the upper airfoil area, C_L is the lift coefficient. Drag force is defined as,

$$F_D = \frac{1}{2} \rho . U_0^{\,2} A . C_D \quad (2)$$

ρ is the density of the fluid flowing in the tunnel, U_0 is the free stream velocity of the fluid flowing in the tunnel, A is the area, C_L is the drag coefficient.

Figure 7. The vertical view of the airfoil in the wind tunnel

EXPERIMENTAL RESULT

In this study, the effect of drag and lift force of 5 synthetic jet actuators placed linearly along the NACA 0020 aircraft wing is examined. Aerodynamic force measurements are made at 50000 Reynolds number (with ±4% uncertainty). Mueller (1999) described MAVs and UAVs as being compatible with flow conditions in this Reynolds number range. The operating frequency applied in the experiment is examined at 2, 4 and 8 Hz using a total of 5 loudspeakers of 4 ohms and 5 Watts. Jet outlets with 2 mm orifice lengths are examined in cylindrical, rectangular, sinusoidal, v-type and inclined rectangles. As reported by Türen and Yavuz (2023), as a result of the experiments conducted at 4 Hz with a fixed pulse width ratio of 1%, flow structures with different orifice geometries are formed at the best flow jet exits. As reported by Genç et all. (2016), the force measurement are measured at 2 ° intervals. Post-stop measurements are made in 1° increments to obtain the necessary data. In this study, in force measurement experiments, lift and drag coefficients are measured at 50000 Reynolds number, between 0º-18º angle of attack, with a 1° measurement interval. Force measurements are made with the loudspeaker on and the loudspeaker off. In these experiments, lift and drag coefficients in different jet geometries and their effects on stall characteristics are investigated by using the loudspeaker as an actuator. The lift (C_L) and drag (C_D) coefficients are calculated and plotted for the attack angle α of the airfoil. In Figure 8, the lift and drag forces on the NACA 0020 airfoil are measured when the loudspeakers are turned off. To provide a reference for comparison, the loudspeaker off condition is defined as basic model. In this case, the repose angle of the NACA 0020 airfoil is approximately 10 degrees. The 10º angle of repose in measurements made with the speaker turned off also supports the baseline measurements in the study of Ethiraj and Pillai (2021). In Figure 8, when the speaker is off, the C_L value is 1.068.

Figure 8, a delay in shifting stall is observed in all synthetic jet orifice models except the inclined rectangular orifice model with linear and spaced synthetic jet actuators. The main reason for this appears to be due to the activated synthetic jet actuator, actuator position and orifice jet structures. The maximum lift coefficient and stall angle shift are observed when close to the leading edge (Guoqing et al., 2016).

In the first step of the presented study, the cylinder orifice model placed in the synthetic jet actuator is activated. It is observed that the increase in the best lift coefficient in the Cylinder orifice synthetic jet actuator occurred at 4 Hz frequency, compared to the loudspeaker actuator off condition, by 8%. In the cylinder orifice, there is an increase in the lift coefficient at frequencies of 2 and 4 Hz, but it is observed that it started to decrease again after the frequency of 8 Hz. The reason for this is that after a certain frequency increase, it causes a loss in lift coefficient due to distortions in the vortex structures that occur at the orifice jet exit. The cylinder orifice is shifted stall angle from 10° to approximately 13° in the synthetic jet actuator array. This means that despite a low increase in the lift coefficient in the cylinder orifice structure, a significant change in the shifted stall angle is observed. In Figure 8b, as the operating frequency increases in the Rectangular orifice synthetic jet actuator, the lift coefficient increases. As a result, a better improvement (about 17%) in the buoyancy coefficient is observed with increasing frequency compared to the cylinder orifice model. This seems to be due to the effect of vortex structures formed at the cylinder and rectangular orifice jet exit. Wang et al. (2017) observed that the vortex area of the rectangular orifice is larger compared to the cylindrical orifice shape. Additionally, a 3° shift in the stall angle was observed in the rectangular orifice synthetic jet actuator array. In the V-type orifice synthetic jet actuator, the coefficient of lift force increases linearly with the stall angle. In Figure 8c, as the operating frequency increased, the lift coefficient increased and it is observed that there is an improvement in the best lift

force (approximately 17%) at 8 Hz. A decrease in the lift coefficient is observed compared to the rectangular orifice. The main reason for this is due to the angular structure of the model, distortions occur in the jet structures formed at the orifice exit. It has been observed that these deteriorations lead to a decrease in the lift coefficient and the angle of stall. In this orifice structure, the stall angle creates a 2° translation. In Figure 8d, a 16% improvement is observed at the highest lift coefficient and 10° angle of attack at 2 Hz operating frequency in the sinusoidal orifice synthetic jet actuator. While the stall angle is only shifted by 1° at 2 Hz, a shift of 4° at 4 Hz and 5° at 8 Hz are observed with increasing frequency. Although the maximum lift force decreased at 4 and 8 Hz, the aircraft wing does not enter the stall immediately after the stall angle and the lift coefficient remains at 1.18 levels. It appears that the lift coefficient curve is horizontal at 4 and 8 Hz and then stalls, due to the disruption of the 'laminar separation bubble' formation on the suction surface of the airfoil at low Reynolds numbers by the synthetic jet actuator. In Figure 8e, it is observed that as the operating frequency increases, the lift force coefficient increases and there is an improvement in the best lift force (about 12%) at 4 Hz.

Although there is an increase in the lift coefficient of the Inclined rectangular orifice model compared to the cylinder orifice model, a smaller improvement (about 12%) is observed compared to the other orifice structure. In this orifice model, similar to the sinusoidal geometric structure, the lift coefficient remained constant for a while before stalling and then stalled. In the Inclined rectangular orifice synthetic jet model, it is observed that there is a translation of 4° at 2 and 4 Hz and 5° at 8 Hz. It has been observed that the synthetic jet mechanism is effective in shifting the stall angle in 5 different synthetic jet orifice models. Guoqing et al. (2016) supports the study that the synthetic jet mechanism created using a speaker jet array is effective in analysing the stall control effects of the airfoil. Thus, with the presented study, higher lift coefficient effects are observed and separation is taken under control.

In the NACA 0020 airfoil, in Figure 9, firstly, when the loudspeaker actuator is closed in the synthetic jet mechanism, the drag coefficient (C_D) increases with the angle of attack. It is observed that the C_D of the NACA 0020 airfoil increased by up to 10 degrees, except for the cylinder orifice model. However, after the stall angle, the drag coefficient gradually increases in all orifice structures. As seen in Figure 11, 4 Hz operating frequency is more effective than 2 Hz operating frequency in reducing the drag coefficient. However, at the 8 Hz operating frequency, it causes irregular fluctuations. The main reason for this is the fluctuations in the flow structures formed in orifice jet models. Especially in inclined rectangular models, unstable fluctuations in the drag coefficient are quite high at 8 Hz operating frequency. This causes a negative effect on the wing. Additionally, in rectangular, V type, inclined rectangular orifice models, it is observed that 2 Hz operating frequency is more effective in pre-stall situations, but 4 Hz operating frequency is more effective after stopping. Among the orifice models in the synthetic jet mechanism, the minimum improvement, called the reduction in drag coefficient, is at 8° angle of attack (about 20%) at 2 Hz of the cylindrical model, while the maximum improvement is sinusoidal at 4 Hz at 8° angle of attack (about 80%) and inclined rectangle at 8 Hz.

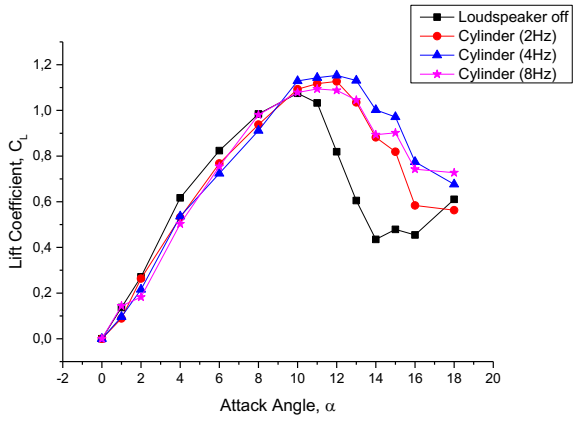

a.

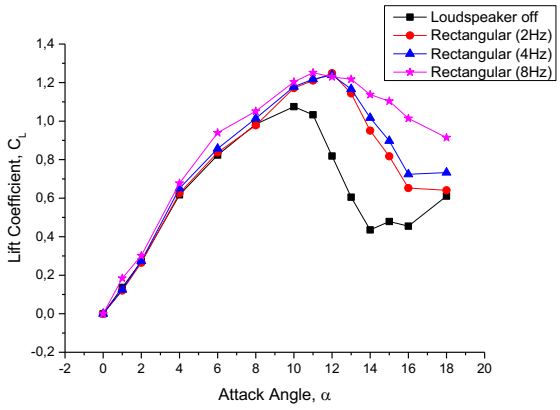

b.

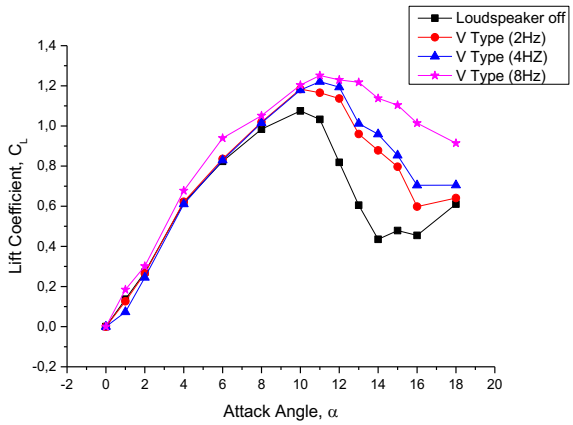

c.

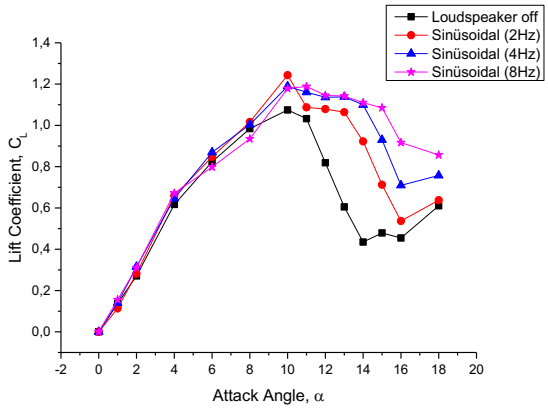

d.

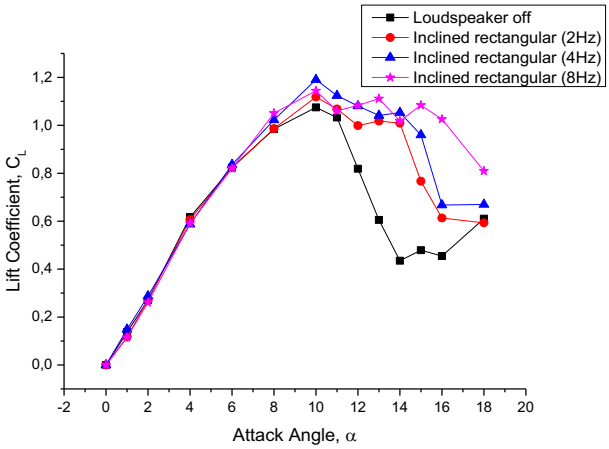

e.

Figure 8. Lift coefficient of the NACA 0020 airfoil synthetic jets at Reynolds number 50 000 **a.** cylinder **b.** Rectangle **c.** Sinusoidal **d.** V type **e.** Inclined rectangular

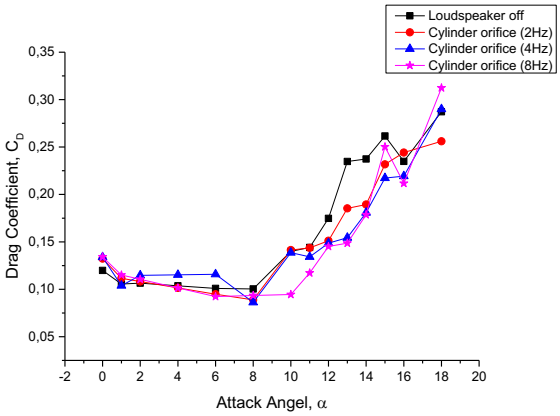

a.

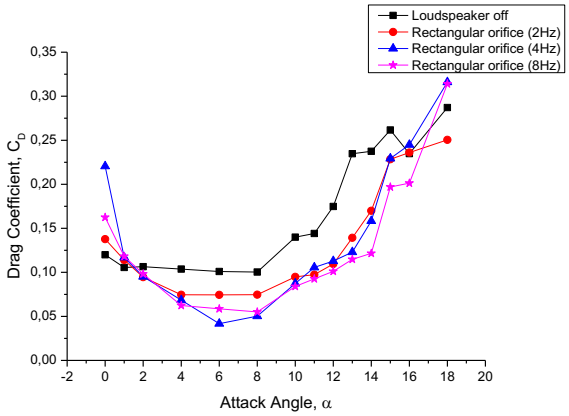

b.

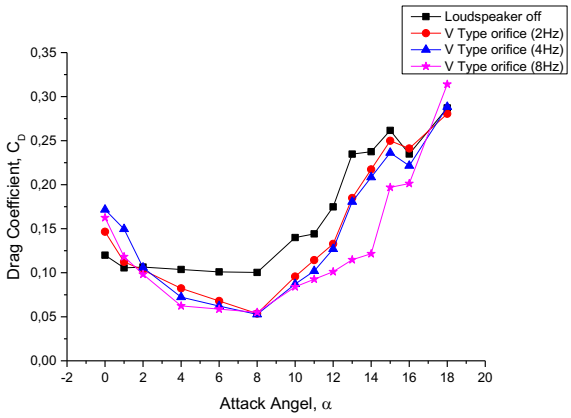

c.

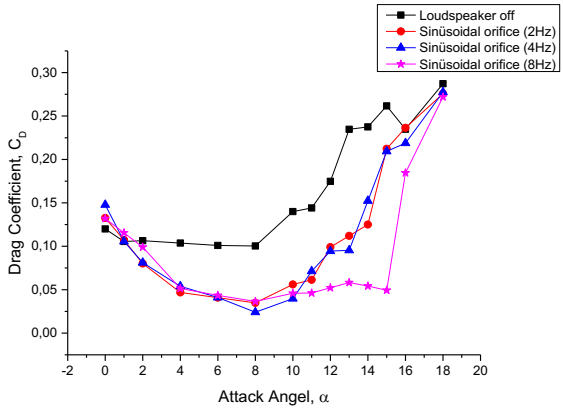

d.

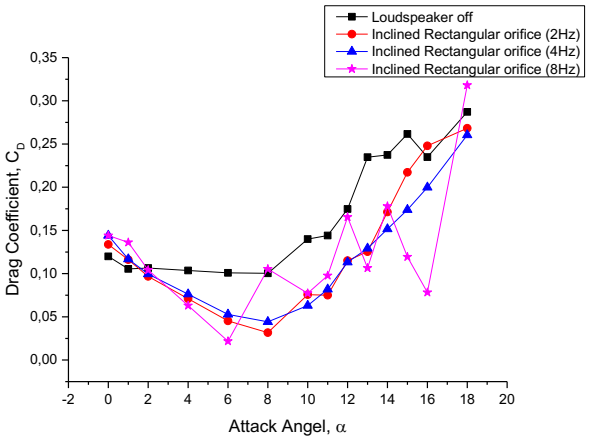

e.

Figure 9. Drag coefficient of the NACA 0020 airfoil synthetic jets at Reynolds number 50 000 **a.** cylinder **b.** Rectangle **c.** Sinusoidal **d.** V type **e.** Inclined rectangular

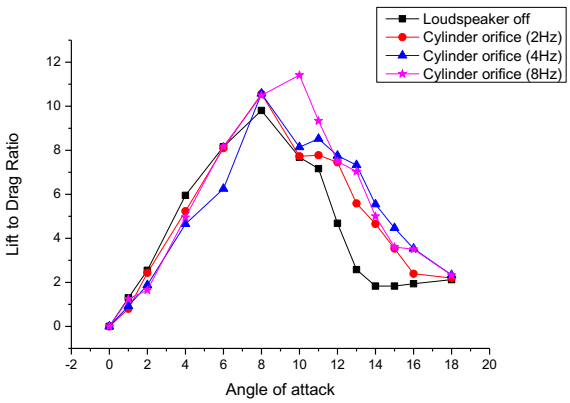

a.

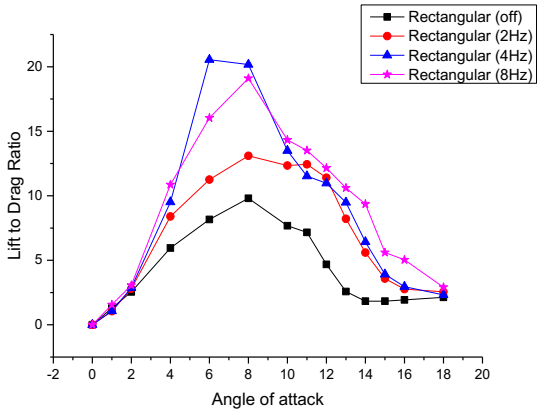

b.

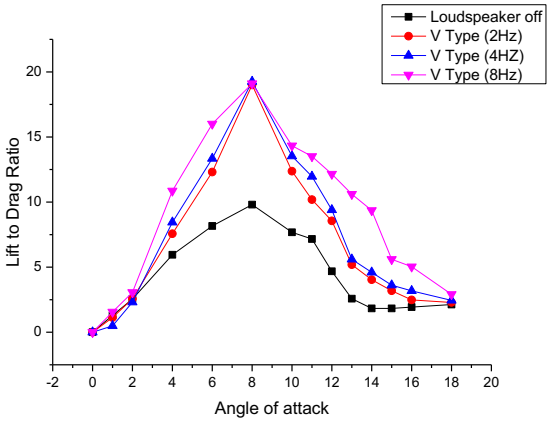

c.

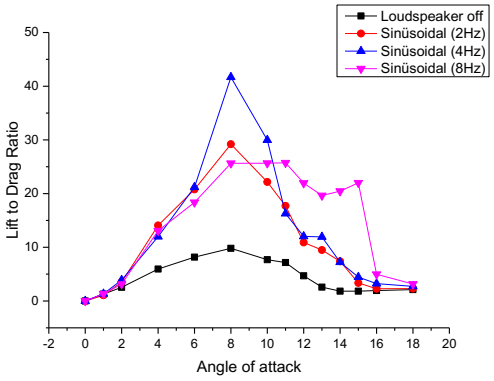

d.

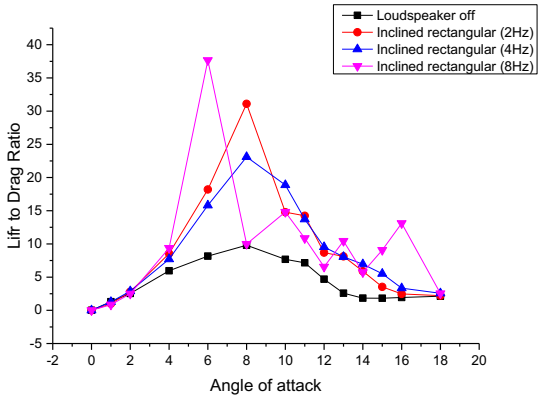

e.

Figure 10. Lift to drag of the NACA 0020 airfoil synthetic jets at Reynolds number 50 000 **a.** cylinder **b.** Rectangle **c.** Sinusoidal **d.** V type **e.** Inclined rectangular

Mueller (1999) observed that the lift and drag coefficient of a smooth airfoil can vary significantly in the range of 10000 to 100000 Reynolds numbers. In the light of these observations, it is observed in our study that the flow in the different orifice synthetic jet mechanism causes shifting in stall, increase in lift coefficient and decrease in drag coefficient.

In this study, it was observed that the different orifice models presented in Figure 9 play a critical role in reducing the drag coefficient. In Figure 10, in the lift-drag ratio graphs of 5 different orifice models in the synthetic jet mechanism, improvements are observed for all models when compared to the basic model with the loudspeaker off. As a result of this study, when the aerodynamic forces are analyzed and interpreted together, different orifice structures have shorter take-off distances and fuel consumption is saved for the same journey. When comparing the loudspeaker off model of the NACA 0020 airfoil with other orifice models, the flight range is extended with improvements in the lift-drag ratio in the aerodynamic design.

To demonstrate the reliability of the lift coefficient at low Reynolds number (Dajun and Takafumi, 2018), the fluctuation of the lift coefficient in a randomly selected time interval is seen in Figure 11. It can be seen that there is a stable fluctuation structure when the loudspeaker is off and the wavelength increases slightly after the stall angle. When orifice models are tested with frequencies of 2, 4 and 8 Hz, it is observed that wavelengths increase with increasing frequency and wavelength frequency increases. Additionally, when the graphs are compared with the lift coefficient graph, it is observed that the periodic oscillation increases after the stall angle in each of them, and these oscillations and the lift coefficient (C_L) fluctuation are directly related to each other.

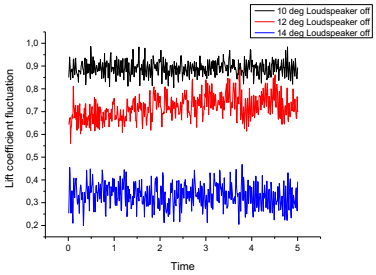
10 deg Loudspeaker off
12 deg Loudspeaker off
14 deg Loudspeaker off
Lift coefficient fluctuation
Time

a.

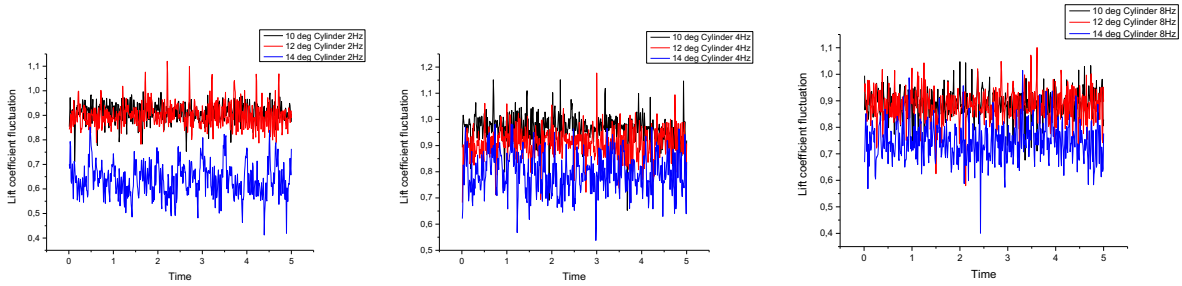
10 deg Cylinder 2Hz
12 deg Cylinder 2Hz
14 deg Cylinder 2Hz
10 deg Cylinder 4Hz
12 deg Cylinder 4Hz
14 deg Cylinder 4Hz
10 deg Cylinder 8Hz
12 deg Cylinder 8Hz
14 deg Cylinder 8Hz
Lift coefficient fluctuation
Time

b.

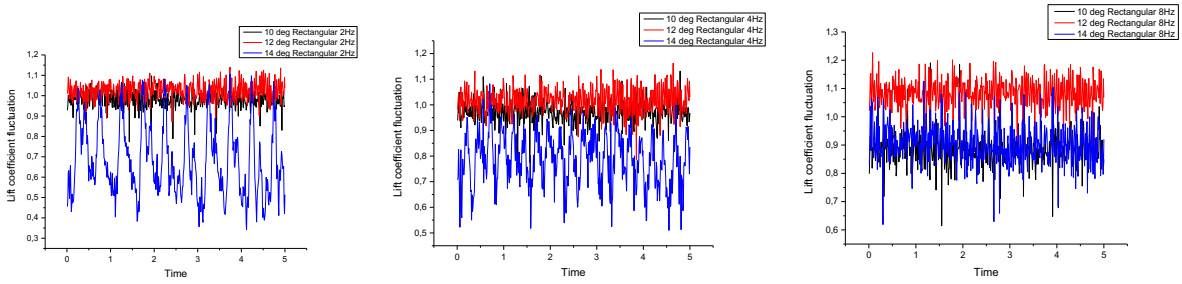
10 deg Rectangular 2Hz
12 deg Rectangular 2Hz
14 deg Rectangular 2Hz
10 deg Rectangular 4Hz
12 deg Rectangular 4Hz
14 deg Rectangular 4Hz
10 deg Rectangular 8Hz
12 deg Rectangular 8Hz
14 deg Rectangular 8Hz
Lift coefficient fluctuation
Time

c.

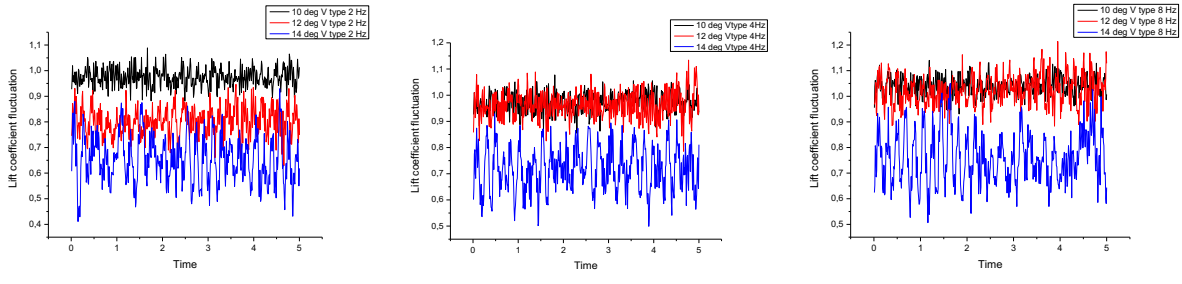
10 deg V type 2 Hz
12 deg V type 2 Hz
14 deg V type 2 Hz
10 deg Vtype 4Hz
12 deg Vtype 4Hz
14 deg Vtype 4Hz
10 deg V type 8 Hz
12 deg V type 8 Hz
14 deg V type 8 Hz
Lift coefficient fluctuation
Time

d.

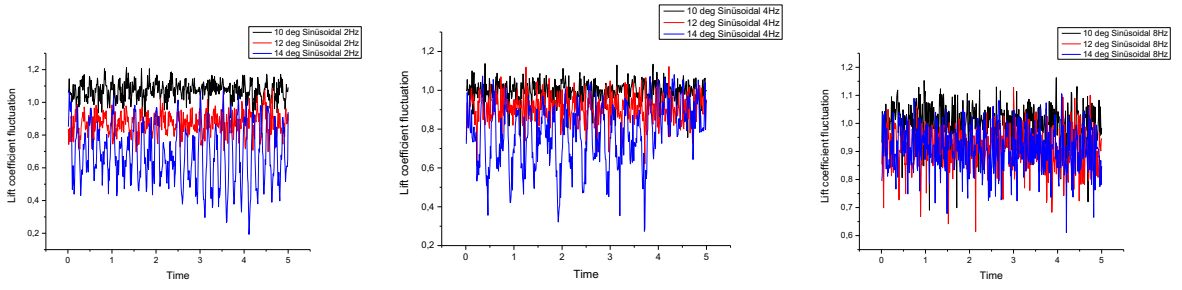
10 deg Sinüsoidal 2Hz
12 deg Sinüsoidal 2Hz
14 deg Sinüsoidal 2Hz
10 deg Sinüsoidal 4Hz
12 deg Sinüsoidal 4Hz
14 deg Sinüsoidal 4Hz
10 deg Sinüsoidal 8Hz
12 deg Sinüsoidal 8Hz
14 deg Sinüsoidal 8Hz
Lift coefficient fluctuation
Time

e.

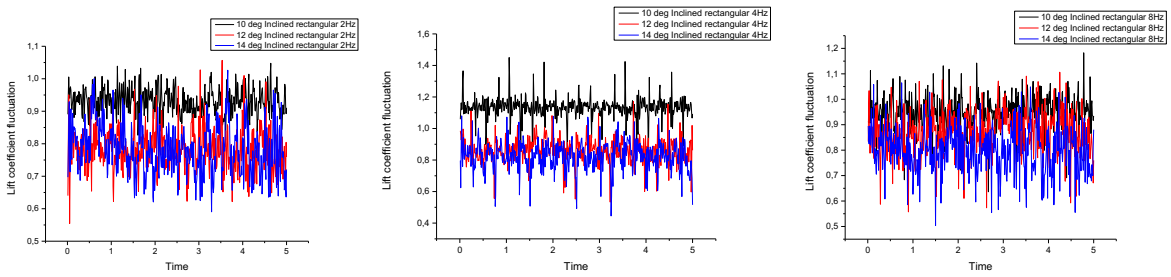

f.

Figure 11. Fluctuating lift coefficient of the NACA 0020 airfoil in closed synthetic jets at Reynolds number 50 000 **a.** Loudspeaker off **b.** Cylinder 2, 4, and 8 Hz **c.** Rectangular 2, 4, and 8 Hz **d.** V type 2, 4, and 8 Hz **e.** Sinusoidal 2, 4, and 8 Hz **f.** Inclined rectangular

CONCLUSIONS

The main objective of this study is to investigate the effects of different orifice geometries on shifting the stall angle in the synthetic jet mechanism. In addition, the effects of different orifice geometries on the airfoils lift coefficient and drag properties are investigated by varying the angle of attack. Based on the presented experimental data, some significant results obtained are as follows:

It has been observed that the use of synthetic jet for flow control has a potential for enhancing the aerodynamic performance. It has been noted that synthetic jet mechanisms based on different orifice geometries have delayed the stall with geometry based differing performance levels.

The orifice geometry, which is most effective in shifting the stall angle, shifted the inclined sinusoidal orifice stall from 10^0 to 14^0 in 4 Hz and from 10^0 to 15^0 in 8 Hz. In addition, it is observed that the stall angles are shifted from 10^0 to 13^0 for cylinder, rectangular, and from 10^0 to 12^0 for V-type orifice structures and from 10^0 to 11^0 for inclined rectangular. According to the results of these experiments, different orifice models have found to be effective in shifting the stall angle.

When the different orifice geometries in the NACA 0020 airfoil are examined, an improvement of approximately 17% in the lift coefficient is observed at 8 Hz and 11^0 angles of attack for the rectangular and V-type orifice models.

In the NACA 0020 airfoil, when stalling occurred, an 80% decrease in the drag coefficient is observed at its maximum value at 8 Hz for the rectangular and sinusoidal models at an angle of attack of 8 degrees, and an outstanding improvement in the drag coefficient is observed. In 8 Hz operation in the inclined rectangular orifice structure, irregularity occurred in the drag coefficient. As a result, this irregularity in the drag force that occurs as the frequency increases has a negative effect on the airfoil.

The study presents results regarding its contribution to the improvements in aerodynamic performance of synthetic jet mechanisms for different orifice geometries on the NACA 0020 airfoil. It contributes to aerodynamic performance by increasing the lift force by approximately 17% and the decrease of drag force by up to 80%. These results contribute to the literature on aerodynamic performance improvements of airfoils in the rapidly developing aircraft industry.

REFERENCES

Andou S. And Ziada S., 2006, Spanwise Characteristics of High-Aspect-Ratio Synthetic jets, *AIAA JOURNAL,* 44(7), 1516-1523

Ahuja K.K. and Burrin R. H., 1984, Control of flow separation by sound, *9 th Aeroacustics Conf. Amerikan Institute of Aeronautics and Astronautics*, Williamsburg, VA

Amitay M., Smith D. R., Kibens V., Parekh D. E., Glazer A., 2001, Aerodynamic flow control over an unconventional airfoil using synthetic jet actuators, *AIAA Journal*, 39(3), 361-370

Babarino S., Bilgen O., Ajaj R. M., Friswell M. I., Inman D. J., 2011, A review of morphing aircraft, *Journal of Intelligent Material Systems and Structures,* 22(9)

Chaudhari M., Bhalchandra P., Agrawal A., 2010, Heat transfer characteristics of synthetic jet impingement cooling, *International Journal of Heat and Mass Transfer,* 53(5–6), 1057-1069

Collins F. G. and Zelenevitz, J., 1975, Influence of sound upon separated flow over wings, *AIAA JOURNAL*. 13(3), 408-410

Crittenden, T., Glezer, A., Funk, R., Parekh, D. 2001, Combustion-driven jet actuators for flow control, *15th AIAA Computational Fluid Dynamics Conference,* Anaheim, California, 2001-2768

Dajun L. and Takafumi N., 2018 Numerical analysis on the oscillation of stall cells over a NACA 0012 aerofoil, *Computers and Fluids,* 175, 246-259

Ethiraj L., Pillai N.S., 2021, Effect of trailling-edge modification over aerodynamic characteristics of NACA 0020 airfoil. *Wind and Structures,* 33(6), 463-470

Feero M. A., Lavoie P. and Sullivan P. E., 2015, Influence of cavity shape on synthetic jet performance, *Sensors and Actuators A: Physical*, 233,1-10

Gad-el-Hak M., 2000, *Flow Control*. by Mohamed Gad-el-Hak, pp. 442. ISBN 0521770068. Cambridge, UK: Cambridge University Press, August

Genç M. S., Karasu İ., Açıkel H. H., 2012, An experimental study on aerodynamics of NACA 2415 aerofoil at low Re numbers., *Experimental Thermal and Fluid Science*, 39, 252-264

Gillarranz J. L., Traub L.W., Rediniotis O. K., 2005, A new class of synthetic jet actuators-Part II: Application to flow separation control, *Journal of Fluids Engineering* 127(2): 377-387

Guoqing Z., Qijun Z., Yunsong G., Xi C., 2016, Experimental investigations for parametric effects of dual synthetic jets on delaying stall of a thick airfoil. *Chinese Journal of Aeronautic,* 29(2): 346-357

Hassan A.A., 2006, A two -point active flow control strategy for improved airfoil stall/post stall aerodynamics. *AIAA JOURNAL*., AIAA-2006-0099

He Y. Y., Cary A. W., Peters D. A., 2001, Parametric and dynamic modeling for synthetic jet control of a post-stall airfoil. Reno/ NV 39th *AIAA Aerospace Science Meeting and Exhibit*, 8-11 January 2001, 0733

Holman R., Galles Q., Carroll., Cattafesta L., 2003, Interaction of adjacent synthetic jet in an airfoil separation control application, *33rd AIAA Fluid Dynamics Conference and Exhibit,* 23-26 June 2003, 2003-3709

Hong, M.H., Cheng, S.Y., Zhong S., 2020, Effect of Geometric Parameters on Synthetic Jet: A review. *Physics of Fluids* 32, 031301

Ingard, U. and Labate, S., 1950, Acoustic Circulation Effects and the Nonlinear Impedance of Orifices. *Journal of the Acoustical Society of America,* 22(2), 211–218

Joshi S. N., Gujarathi Y. S., 2016, A Review on Active and Passive Flow Control Techniques, *International Journal on Recent Technologies in Mechanical and Electrical Engineering,* 3(4)

Kim S. H., Kim C., 2009, Separation control on NACA 23012 using synthetic jet, *Aerospace Science Technology*, 13,172-182

Lee B, Kim M, Lee J, Kim C., 2012, Separation control characteristics of synthetic jets with circular exit array. *AIAA Flow Control Conference*, New Orleans, AIAA-2012-3050

Mohsen J., 2011, *Laminar separation buble: Its structure, dynamics and control.* Charmers University. of Tecnology. Gothenburg, Sweeden

Mallinson S.G., Reizes J.A., Hong G., Westbury P.S., 2004, Analysis of hot-wire anemometry data obtained in a synthetic jet flow. *Experimental Thermal and Fluid Science* 28, 265–272

Mueller T. J., 1999*, Aerodynamic Measurements at Low Reynolds Numbers for Fixed Wing Micro-Air Vehicles. Development and Operation of UAVs for Military and Civil Applications*, Hessert Center for Aerospace Research, University of Notre Dame, 8.1-8.32

Paula A. A., Kleine V. G., Porto F. M., 2017, The Thickness Effect on Symmetrical Airfoil Flow Characteristics at low Reynolds number, *55th AIAA Aerospace Sciences Meeting*, 2017-1422

Qingfeng X. and Zhong S., 2013, Liquids mixing enhanced by multiple synthetic jet pairs at low Reynolds numbers, *Chemical Engineering Science*, 102, 10-23

Seifert A., Darabi A., Wyganski I., 1996, Delay of airfoil stall by periodic excitation, *Journal of Aircraft*, 33(4), 691–698

Smith B. L., and Glezer A., 1998, The Formation and Evolution of Synthetic Jets. *Physics of Fluids* 10 (9): 2281–2297

Traub L., Miller A. and Rediniotis O., 2004, Effect of Synthetic jets of actuation on a ramping NACA 0015 airfol, Journal of Aircraft,41(5), 1153-1162

Trávníček Z., Vogel J., Vít T., Maršík F., 2005, Flow field and mass transfer experimental and numerical studies of a synthetic impinging jet. *In: Proc. 4th International Conference on Heat Transfer, Fluid Mechanics and Thermodynamics (HEFAT2005)*, Cairo, Egypt, No. ZT4

Türen E., & Yavuz H., 2023, Schlieren imaging investigation of flow fields in synthetic jets generated by different orifice geometries with varying aspect ratios, *Journal of Visualization*, 26(4), 851-874.

Wang L., Feng L.H., Wang J.-J., Li T., 2017, Parameter influence on the evolution of low-aspect-ratio rectangular synthetic jets, Journal of. Visualization, 21, 105

Yarusevych, S., Kawall, J. G., and Sullivan, P. E., 2003, Effect of acoustic excitation on airfoil performance at low Reynolds numbers, *AIAA JOURNAL*. 41(8),1599-1601

Yen J., Ahmed N. A., 2012, Parametric study of dynamic stall flow field with synthetic jet actuation, *Journal of Fluids Engineering*, 134, 071106(1-8)

You D., Moin P., 2008, Active control of flow separation over an airfoil using synthetic jets, *Journal of Fluids and Structures*, 24,1349-1357

Youmin Y., Simon T W., Zhang M., Yeom T., North M. T., Cui T., 2014, Enhancing heat transfer in air-cooled heat sinks using piezoelectrically-driven agitators and synthetic jets. *International Journal of Heat and Mass Transfer*, 68, 184-193

Zaman K. B. M.Q., and McKinzie D. J., 1991, Control of laminar separation over airfoil by acoustic axcition. *AIAA JOURNAL*, 29(7), 1075-1083

Zhang S., Zhong S., 2009, Experimental investigation of flow separation control using an array of synthetic jets. 39th *AIAA Fluid Dynamics Conference*, San Antonio, Texas, 22 25 June

Zhang D., Yang K., Cheng Q.H., Gao J., 2015, Numerical investigation of heat transfer performance of synthetic jet impingement onto dimpled/protrusioned surface. *Thermal Science* 19 (1), 221-229

Zhao G., Zhao Q., Yunsong G., Xi C., 2016, Experimental investigations for parametric effects of dual synthetic jets on delaying stall of a thick airfoil. *Chinese Journal of Aeronautics*, 29(2), 346-357

Authors

Esra TÜREN, received her B.Sc. degree and M.Sc. degree in Mechanical Engineering from Süleyman Demirel University, Isparta, Turkey in 2013 and 2015, respectively. She is currently a PhD student at Çukurova University. Her research interests for flow control and flow control applications.

Hakan YAVUZ, received his B.Sc. degree in mechanical engineering from Gazi University, Ankara, Turkey and the M.Sc. and Ph.D. degrees in mechatronics engineering from the Lancaster University,Lancaster, U.K., respectively. His current research interests include active flow control, robotic systems, development of intelligent control, design and development of mechatronic systems, renewable energy systems, modeling and analysis of engineering systems, input shaping for residual vibration elimination, and wave energy converters and related control applications.